RESEARCH REPORTS

THE EFFECT OF FLAT SHAFT ON THE UNSTABLE VIBRATIONS OF A SHAFT CARRYING AN UNSYMMETRICAL ROTOR

(Part I. Analytical treatment)

TOSHIO YAMAMOTO, HIROSHI ŌTA and KAZUTOYO KŌNO

Department of Mechanical Engineering

(Received July 12, 1968)

1. Introduction

When two principal moments of inertia I_1, I_2 about the axes perpendicular to the rotating axis of a rotor are unequal, *i.e.* $I_1 \neq I_2$, the rotor is called an "unsymmetrical rotor". It has been reported by the authors that in a rotating shaft system carrying an unsymmetrical rotor, there are two kinds of unstable regions in the neighborhood of both the major critical speed ω_c[1][2] and the rotating speed ω_d at which the sum of two natural frequencies p_1+p_2 is equal to twice rotating speed of the shaft $2\omega_d$[3]. In 1961, S. H. Crandall and P. J. Brosens discussed the interaction through gyroscopic coupling between the inertia and stiffness inequalities for unstable vibrations referring to the inclination angles θ_x, θ_y of the rotor, which occur in the neighborhood of the major critical speed ω_c[4].

In the present paper, a vibratory system of four-degree-of-freedom consisting of a rotating shaft with an unsymmetrical flexibility and an unsymmetrical rotor is treated, in which the deflections x, y and the inclination angles θ_x, θ_y of the rotor couple each other through gyroscopic terms; and a quantitative analysis for the unstable vibrations in the neighborhood of both ω_c and ω_d is derived, and the simultaneous effects of the diametral inertia inequality of the rotor and the unsymmetrical stiffness of the shaft on the unstable vibrations are explicitly appreciated.

2. Equations of Motion

Let the polar moment of inertia about the rotating axis of the rotor be I_p; other two principal moments of inertia be I_1, I_2 $(I_1>I_2)$; the deflection of the center M of the rotor be x, y; the inclination angles of the rotor be θ_x, θ_y: the damping coefficient for $\dot{x}$, $\dot{y}$ and $\dot{\theta}_x$, $\dot{\theta}_y$ be c_1 and c_2 respectively; the mass of the rotor W/g, the rotating speed of the shaft ω, the spring constants of the shaft having unequal stiffness be $\alpha\pm\Delta\alpha$, $\gamma\pm\Delta\gamma$ and $\delta\pm\Delta\delta$ which are measured in the direction of the principal axes of shaft cross section; the angle between the principal axis of stiffness MY_3 which coincides with the direction of $\alpha-\Delta\alpha$ etc. and the principal axis of moment of inertia MY_2 (*i.e.* the direction of I_1) be ζ;

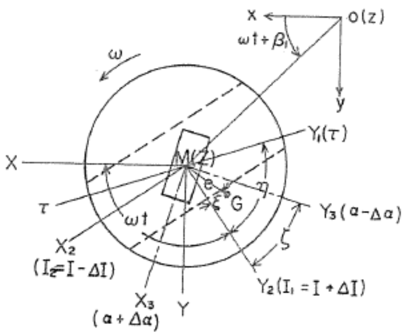

FIG. 1

the direction $\vec{MG}$ of the eccentricity e measured from the axis MY_2 be ξ; the direction $\vec{MY_1}$ of the dynamic unbalance τ measured from MY_2 be η (see Fig. 1). Introducing the mean value of diametral moment of inertia $I=(I_1+I_2)/2$, the inertia asymmetry $\Delta I=(I_1-I_2)/2$ and the dimensionless quantities

$$\left.\begin{array}{l} I_p/I=i_p,\ \ \Delta I/I=\Delta,\ x/\sqrt{Ig/W}=x',\ y/\sqrt{Ig/W}=y',\ e/\sqrt{Ig/W}=e', \\ t\sqrt{\alpha g/W}=t',\ \omega/\sqrt{\alpha g/W}=\omega',\ \gamma\sqrt{W/(Ig)}/\alpha=\gamma',\ \delta W/(\alpha I g)=\delta', \\ c_1/\sqrt{W\alpha/g}=c_1',\ c_2\sqrt{W/(\alpha g)}/I=c_2',\ \Delta\alpha/\alpha=\Delta_{11},\ \Delta\gamma/\gamma=\Delta_{12},\ \Delta\delta/\delta=\Delta_{22} \end{array}\right\} \quad (1)$$

and further omitting primes on the dimensionless quantities for brevity, the following equations of motion for the unsymmetrical rotor carried by the rotating shaft with unequal stiffness are derived:

$$\left.\begin{array}{l} \ddot{x}+c_1\dot{x}+x+\gamma\theta_x-\Delta_{11}\{x\cos(2\omega t+2\zeta)+y\sin(2\omega t+2\zeta)\}-\gamma\Delta_{12}\{\theta_x\cos(2\omega t+2\zeta) \\ \qquad +\theta_y\sin(2\omega t+2\zeta)\}=e\omega^2\cos(\omega t+\xi) \\ \ddot{y}+c_1\dot{y}+y+\gamma\theta_y-\Delta_{11}\{x\sin(2\omega t+2\zeta)-y\cos(2\omega t+2\zeta)\}-\gamma\Delta_{12}\{\theta_x\sin(2\omega t+2\zeta) \\ \qquad -\theta_y\cos(2\omega t+2\zeta)\}=e\omega^2\sin(\omega t+\xi) \\ \ddot{\theta}_x+i_p\omega\dot{\theta}_y+c_2\dot{\theta}_x+\gamma x+\delta\theta_x-\Delta\cdot\dfrac{d}{dt}(\dot{\theta}_x\cos 2\omega t+\dot{\theta}_y\sin 2\omega t)-\gamma\Delta_{12}\{x\cos(2\omega t+2\zeta) \\ \qquad +y\sin(2\omega t+2\zeta)\}-\delta\Delta_{22}\{\theta_x\cos(2\omega t+2\zeta)+\theta_y\sin(2\omega t+2\zeta)\} \\ \qquad =\tau\omega^2\{(i_p-1)\cos(\omega t+\eta)-\Delta\cos(\omega t-\eta)\} \\ \ddot{\theta}_y-i_p\omega\dot{\theta}_x+c_2\dot{\theta}_y+\gamma y+\delta\theta_y-\Delta\cdot\dfrac{d}{dt}(\dot{\theta}_x\sin 2\omega t-\dot{\theta}_y\cos 2\omega t)-\gamma\Delta_{12}\{x\sin(2\omega t+2\zeta) \\ \qquad -y\cos(2\omega t+2\zeta)\}-\delta\Delta_{22}\{\theta_x\sin(2\omega t+2\zeta)-\theta_y\cos(2\omega t+2\zeta)\} \\ \qquad =\tau\omega^2\{(i_p-1)\sin(\omega t+\eta)-\Delta\sin(\omega t-\eta)\} \end{array}\right\} \quad (2)$$

Equations of motion for a symmetrical rotor mounted by a shaft with unequal stiffness[1) 2)] and an unsymmetrical rotor carried by a circular shaft[1) 3)] are obtained by putting $\Delta=0$, $\zeta=0°$ and $\Delta_{ij}=0$ in Eq. (2) respectively.

3. Forced Vibrations

3.1. Solutions of forced vibrations

Forced vibrations induced by e and τ are represented by

$$\left.\begin{aligned} \begin{matrix} x \\ y \end{matrix} &= E^{\cos}_{\sin}(\omega t+\beta_1) = A^{\cos}_{\sin}\omega t \mp B^{\sin}_{\cos}\omega t, \\ \begin{matrix} \theta_x \\ \theta_y \end{matrix} &= F^{\cos}_{\sin}(\omega t+\beta_2) = C^{\cos}_{\sin}\omega t \mp D^{\sin}_{\cos}\omega t \end{aligned}\right\} \tag{3}$$

where β_1, β_2 are phase differences between vibrations and the axis MY_2. It is readily seen from Eq. (3), (4) that if the cofactor of the determinant

$$|a_{ij}| = \begin{vmatrix} 1-\omega^2-\Delta_{11}\cos 2\zeta & -\Delta_{11}\sin 2\zeta - c_1\omega & \gamma(1-\Delta_{12}\cos 2\zeta) & -\gamma\Delta_{12}\sin 2\zeta \\ -\Delta_{11}\sin 2\zeta + c_1\omega & 1-\omega^2+\Delta_{11}\cos 2\zeta & -\gamma\Delta_{12}\sin 2\zeta & \gamma(1+\Delta_{12}\cos 2\zeta) \\ \gamma(1-\Delta_{12}\cos 2\zeta) & -\gamma\Delta_{12}\sin 2\zeta & \begin{matrix}\delta(1-\Delta_{22}\cos 2\zeta) \\ +(i_p-1-\Delta)\omega^2\end{matrix} & -\delta\Delta_{22}\sin 2\zeta - c_2\omega \\ -\gamma\Delta_{12}\sin 2\zeta & \gamma(1+\Delta_{12}\cos 2\zeta) & -\delta\Delta_{22}\sin 2\zeta + c_2\omega & \begin{matrix}\delta(1+\Delta_{22}\cos 2\zeta) \\ +(i_p-1+\Delta)\omega^2\end{matrix} \end{vmatrix} \tag{4}$$

is denoted by A_{ij}, the amplitudes of forced vibrations A, B, C, D are given by the following equation:

$$|a_{ij}|\begin{pmatrix} A \\ B \\ C \\ D \end{pmatrix} = (A_{ji})\begin{pmatrix} e\omega^2\cos\xi \\ e\omega^2\sin\xi \\ \tau\omega^2(i_p-1-\Delta)\cos\eta \\ \tau\omega^2(i_p-1+\Delta)\sin\eta \end{pmatrix} \tag{5}$$

3.2. Unstable regions of forced vibrations

In this section a simple case of $\Delta_{11}=\Delta_{12}=\Delta_{22}=\Delta_s$, *i.e.* the case of a "flat shaft" is considered, which occurs if the shaft with unequal stiffness has an uniform cross section.

When the orientation ζ is equal to 0° or 90° and $c_1=c_2=0$, the vanishing denominators in the equations of the amplitudes A, C and B, D results in the following major critical speeds ω_{c21}, ω_{c11} and ω_{c22}, ω_{c12} separately: For the case of $\zeta=90°$

$$\left.\begin{aligned} \begin{matrix}\omega^2_{c21} \\ \omega^2_{c11}\end{matrix} &= \frac{(1+\Delta_s)\{(i_p-1-\Delta-\delta) \pm \sqrt{(i_p-1-\Delta+\delta)^2-4(i_p-1-\Delta)\gamma^2}\}}{2(i_p-1-\Delta)} \\ \begin{matrix}\omega^2_{c22} \\ \omega^2_{c12}\end{matrix} &= \frac{(1-\Delta_s)\{(i_p-1+\Delta-\delta) \pm \sqrt{(i_p-1+\Delta+\delta)^2-4(i_p-1+\Delta)\gamma^2}\}}{2(i_p-1+\Delta)} \end{aligned}\right\} \tag{6}$$

For case of $\zeta=0°$, the sign of Δ_s in Eq. (6) must be changed. It suggests that the magnitudes of the major critical speeds vary according to the value of the orientation ζ.

In the range of $|a_{ij}|<0$ the forced vibrations become statically unstable[1)2)], and the boundary rotating speeds furnished by $|a_{ij}|=0$ coincide with the major critical speeds of Eq. (6). Accordingly there are two static unstable regions, *i.e.* the lower region $\omega_{c21}\sim\omega_{c22}$ and the higher region $\omega_{c11}\sim\omega_{c12}$[1)].

Simultaneous effects of the asymmetry Δ of the rotor and the unsymmetrical shaft stiffness Δ_s will be discussed. The unstable regions are changed with the value of ζ as shown in Figs. 2 (a), (b), (c). Fig. 2 shows that elimination of the unstable region can be realized by means of an appropriate combination of Δ and Δ_s. The couple of curves when $\zeta=90°$ in Fig. 2 (a) cross each other in the neighborhood of $\Delta=0.25$. It shows that the unstable region vanishes even when $c_1=c_2=0$. The following condition for elimination of the unstable region is derived by putting $\omega_{c21}=\omega_{c22}$ or $\omega_{c11}=\omega_{c12}$ in Eq. (6):

$$\frac{1+\Delta_s}{1-\Delta_s}=g(\Delta)=\frac{(i_p-1-\Delta)\{(i_p-1+\Delta-\delta)\pm\sqrt{(i_p-1+\Delta+\delta)^2-4(i_p-1+\Delta)\gamma^2}\}}{(i_p-1+\Delta)\{(i_p-1-\Delta-\delta)\pm\sqrt{(i_p-1-\Delta+\delta)^2-4(i_p-1-\Delta)\gamma^2}\}} \tag{7}$$

Eq. (7) for $\Delta_s=0.1$ and the upper sign results in $\Delta=0.2487$ which agrees with the result shown in Fig. 2 (a). For comparison the major critical speeds of the circular shaft system (*i.e.* $\Delta_s=0$) with $\Delta=0.322$ are indicated by the symbol ○ in Fig. 2 (a). As is seen in Fig. 2, the unstable region become smaller with increasing of the damping, and finally they vanish for somewhat small asymmetry Δ as shown in Fig. 2 (c).

3.3. The response curves in the neighborhood of the major critical speed

Since there is no unstable region when $\Delta=0.322$, $\Delta_s=0.1$, $c_1=c_2=0.1$ as shown in Fig. 2 (c), the steady forced vibrations induced by e and τ occur in the neighborhood of the major critical speed ω_c. The amplitudes E of deflection indced by e

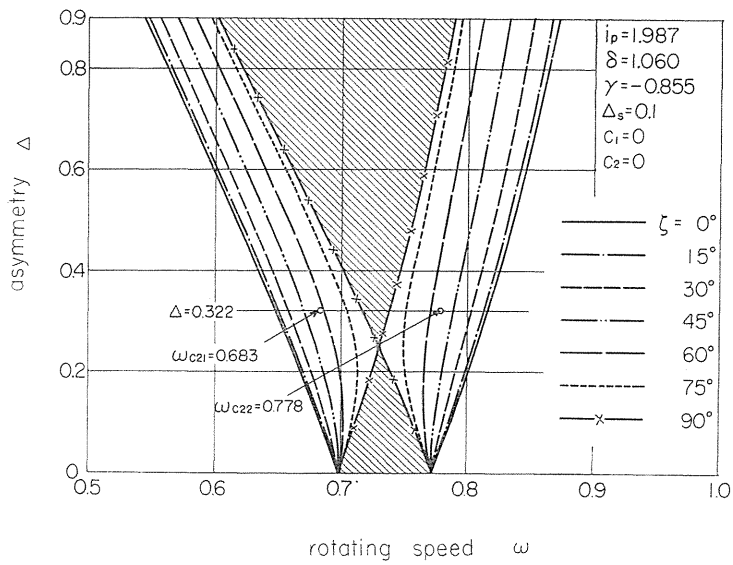

(a) $c_1=c_2=0$

FIG. 2. Unstable region btween ω_{c21} and ω_{c22}.

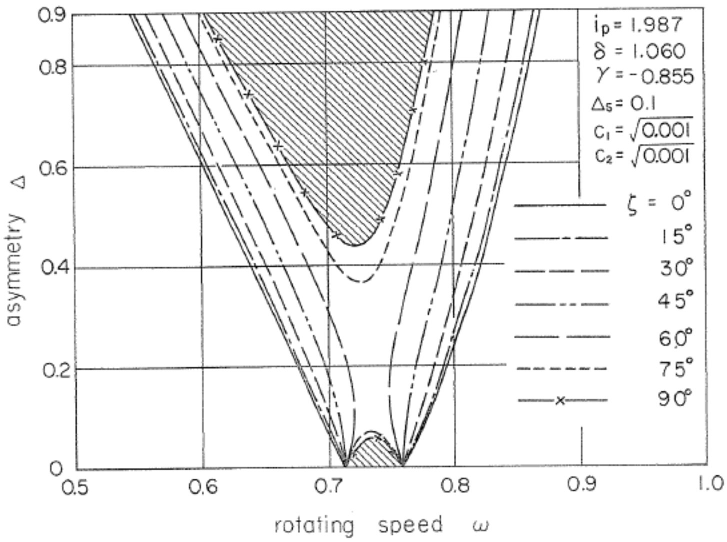

(b) $c_1 = c_2 = \sqrt{0.001}$

FIG. 2. Unstable region between ω_{c21} and ω_{c22}.

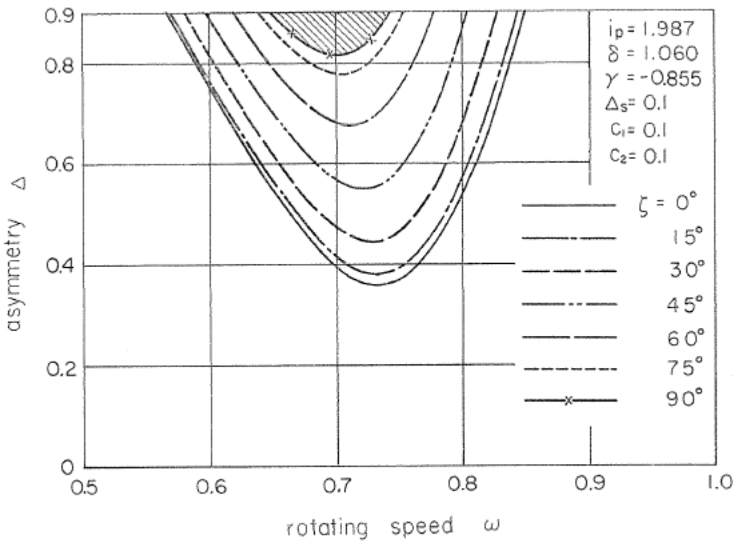

(c) $c_1 = c_2 = 0.1$

FIG. 2. Unstable region between ω_{c21} and ω_{c22}.

and τ are shown by Figs. 3 (a) and (b) severally. Similar response curves are obtained for the amplitudes F of inclination. The maximum values of amplitude E are plotted against the orientation ζ for case of $\xi, \eta = 0°, 45°, 90°, -45°$ in Figs. 4 (a), (b). For comparison, the maximum amplitudes E for the system with $\Delta = 0$ and $\Delta_s = 0$ are indicated by the broken line curves in Fig. 4.

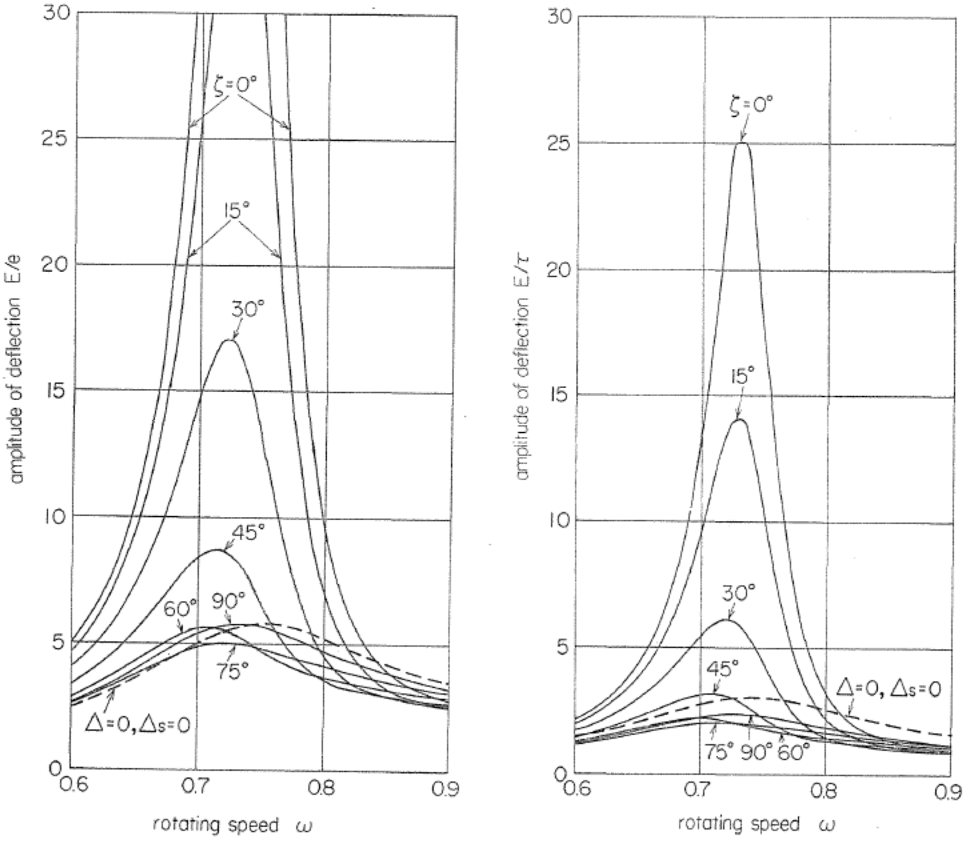

(a) $E/e-\omega$ $(\xi=0°)$ (b) $E/\tau-\omega$ $(\eta=0°)$

$i_p=1.987,\ \delta=1.060,\ \gamma=-0.855,\ \Delta=0.322,\ \Delta_s=0.1,\ c_1=c_2=0.1$

FIG. 3. Response curve at ω_{c2}.

4. Free Vibration

4.1. Frequency equation and the unstable region

Since the asymmetry Δ of the rotor and the unsymmetrical shaft stiffness Δ_s result in coexistence of two free vibrations with frequencies p and $\bar{p}=2\omega-p$ for each degree of freedom, the free vibrations should be represented by

$$\left.\begin{aligned} \begin{matrix} x \\ y \end{matrix} &= A\begin{matrix}\scriptstyle\cos\\ \scriptstyle\sin\end{matrix} pt \mp B\begin{matrix}\scriptstyle\sin\\ \scriptstyle\cos\end{matrix} pt + \bar{A}\begin{matrix}\scriptstyle\cos\\ \scriptstyle\sin\end{matrix} \bar{p}t \mp \bar{B}\begin{matrix}\scriptstyle\sin\\ \scriptstyle\cos\end{matrix} \bar{p}t, \\ \begin{matrix} \theta_x \\ \theta_y \end{matrix} &= C\begin{matrix}\scriptstyle\cos\\ \scriptstyle\sin\end{matrix} pt \mp D\begin{matrix}\scriptstyle\sin\\ \scriptstyle\cos\end{matrix} pt + \bar{C}\begin{matrix}\scriptstyle\cos\\ \scriptstyle\sin\end{matrix} \bar{p}t \mp \bar{D}\begin{matrix}\scriptstyle\sin\\ \scriptstyle\cos\end{matrix} \bar{p}t \end{aligned}\right\} \tag{8}$$

Substituting Eq. (8) into Eq. (2) and putting $e=\tau=0$, $c_1=c_2=0$, the following equation $\Phi=0$ is obtained:

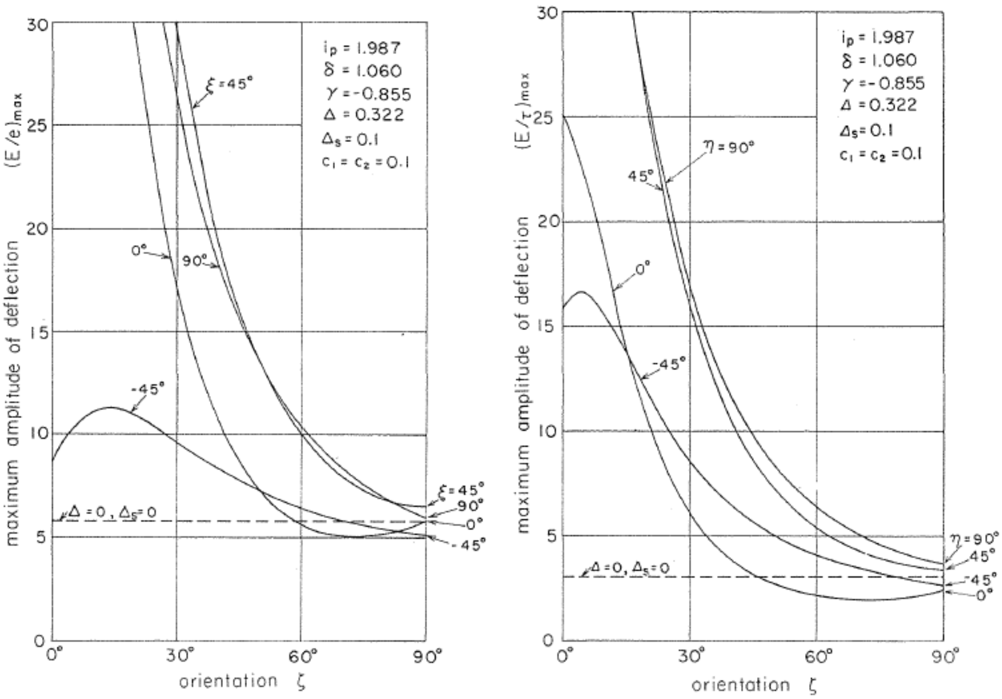

(a) $(E/e)_{\max}-\zeta$ diagram (b) $(E/\tau)_{\max}-\zeta$ diagram

FIG. 4. The relation between the maximum amplitude of deflection and the orientation ζ at ω_{c2}.

$$\Phi=\begin{vmatrix}
H & \gamma & \Delta_{11}\cos 2\zeta & \gamma\Delta_{12}\cos 2\zeta & \Delta_{11}\sin 2\zeta & \gamma\Delta_{12}\sin 2\zeta & 0 & 0 \\
\gamma & G & \gamma\Delta_{12}\cos 2\zeta & \Delta_{p\bar{p}}+\delta\Delta_{22}\cos 2\zeta & \gamma\Delta_{12}\sin 2\zeta & \delta\Delta_{22}\sin 2\zeta & 0 & 0 \\
\Delta_{11}\cos 2\zeta & \gamma\Delta_{12}\cos 2\zeta & \overline{H} & \gamma & 0 & 0 & -\Delta_{11}\sin 2\zeta & -\gamma\Delta_{12}\sin 2\zeta \\
\gamma\Delta_{12}\cos 2\zeta & \Delta_{p\bar{p}}+\delta\Delta_{22}\cos 2\zeta & \gamma & \overline{G} & 0 & 0 & -\gamma\Delta_{12}\sin 2\zeta & -\delta\Delta_{22}\sin 2\zeta \\
\Delta_{11}\sin 2\zeta & \gamma\Delta_{12}\sin 2\zeta & 0 & 0 & \overline{H} & \gamma & \Delta_{11}\cos 2\zeta & \gamma\Delta_{12}\cos 2\zeta \\
\gamma\Delta_{12}\sin 2\zeta & \delta\Delta_{22}\sin 2\zeta & 0 & 0 & \gamma & \overline{G} & \gamma\Delta_{12}\cos 2\zeta & \Delta_{p\bar{p}}+\delta\Delta_{22}\cos 2\zeta \\
0 & 0 & -\Delta_{11}\sin 2\zeta & -\gamma\Delta_{12}\sin 2\zeta & \Delta_{11}\cos 2\zeta & \gamma\Delta_{12}\cos 2\zeta & H & \gamma \\
0 & 0 & -\gamma\Delta_{12}\sin 2\zeta & -\delta\Delta_{22}\sin 2\zeta & \gamma\Delta_{12}\cos 2\zeta & \Delta_{p\bar{p}}+\delta\Delta_{22}\cos 2\zeta & \gamma & G
\end{vmatrix}=0 \tag{9}$$

Some calculation shows that Eq. (9) can be represented by the form $\Phi=\Phi'^2=0$ with

$$\begin{aligned}
\Phi' = ff' + [& -\Delta_{11}^2 G\overline{G} - \gamma^2\Delta_{12}^2(H\overline{G}+\overline{H}G) - \delta^2\Delta_{22}^2 H\overline{H} + 2\gamma^2\Delta_{11}\Delta_{12}(G+\overline{G}) \\
& + 2\delta\gamma^2\Delta_{12}\Delta_{22}(H+\overline{H}) - 2(\delta\Delta_{11}\Delta_{22}+\gamma^2\Delta_{12}^2)\gamma^2 - \Delta^2 p^2\bar{p}^2 H\overline{H} + 2\Delta p\bar{p} \\
& \{-\gamma^2\Delta_{11}+\gamma^2\Delta_{12}(H+\overline{H}) - \delta\Delta_{22}H\overline{H}\}\cos 2\zeta] \\
& + \{(\delta\Delta_{11}\Delta_{22}-\gamma^2\Delta_{12}^2)^2 + \Delta^2\Delta_{11}^2 p^2\bar{p}^2 + 2\Delta\Delta_{11}p\bar{p}(\delta\Delta_{11}\Delta_{22}-\gamma^2\Delta_{12}^2)\cos 2\zeta\} = 0
\end{aligned} \tag{10}$$

in which $H=1-p^2$, $\overline{H}=1-\bar{p}^2$, $G=\delta+i_p\omega p-p^2$, $\overline{G}=\delta+i_p\omega\bar{p}-\bar{p}^2$, $f=HG-\gamma^2$ and $\bar{f}=\overline{H}\overline{G}-\gamma^2$. When $\Delta=0$ and $\Delta_{ij}=0$, Eq. (10) reduces to $\Phi'=f\bar{f}=0$. The unstable vibrations take place in the neighborhood of the intersecting points of the curves $f=0$ and $\bar{f}=0$ provided that Δ and Δ_{ij} are somewhat small[1)2)3)]. Accordingly the nature of Eq. (10) in the neighborhood of these intersecting points will be discussed. Since $f=0$ and $\bar{f}=0$ are simultaneously held in this intersecting point, *i.e.*, $HG=\bar{H}\bar{G}=\gamma^2$, Φ' in Eq. (10) reduces to

$$\Phi' = f\bar{f} - \varphi_2/(H\bar{H}) + \varphi_4 = 0 \tag{11}$$

where

$$\left.\begin{aligned} \varphi_2 &= Q^2 + R^2 + 2QR\cos 2\zeta \geqq (|Q| - |R|)^2 \geqq 0 \\ \varphi_4 &= S^2 + T^2 + 2ST\cos 2\zeta \geqq (|S| - |T|)^2 \geqq 0 \end{aligned}\right\} \tag{12-a}$$

$$\left.\begin{aligned} Q &= \gamma^2\Delta_{11} - \gamma^2\Delta_{12}(H+\bar{H}) + \delta\Delta_{22}H\bar{H}, \quad R = \Delta p\bar{p}H\bar{H}, \\ S &= \delta\Delta_{11}\Delta_{22} - \gamma^2\Delta_{12}^2, \quad T = \Delta\Delta_{11}p\bar{p}. \end{aligned}\right\} \tag{12-b}$$

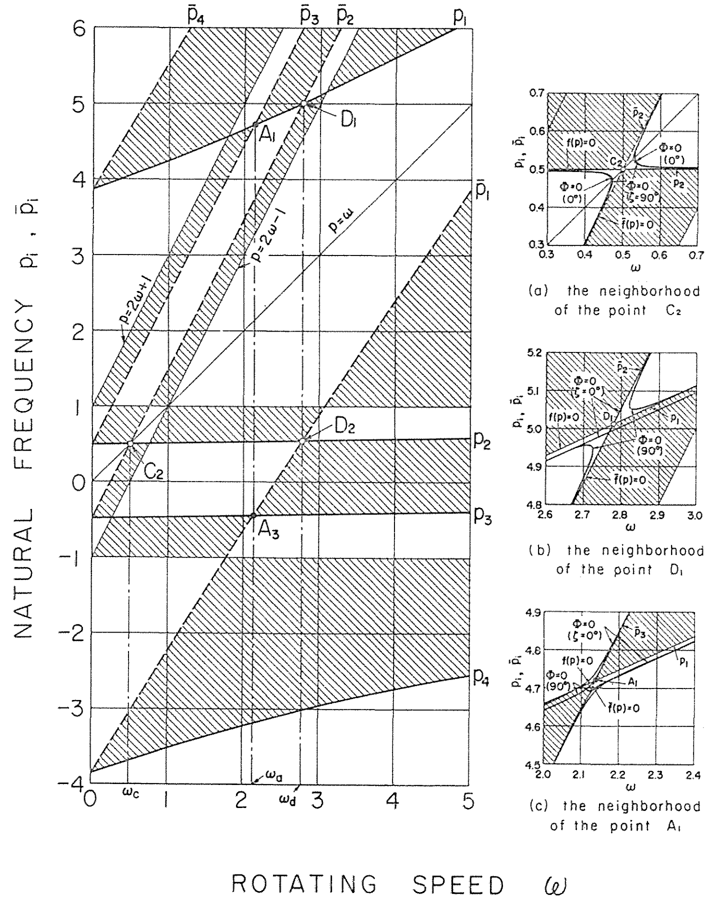

FIG. 5. The relation between the roots of $f=0$, $\bar{f}=0$ and the rotating speed ω. (Experiment IV, $i_p=0.7536$, $\delta=14.1786$, $\gamma=-3.2525$, $\sqrt{\alpha g/W}=441.9$ rpm)

It should be noted from Eq. (12-a) that φ_2 and φ_4 take always the positive values or zero. Under the assumption that the fourth power term of Δ, Δ_{ij} in Eq. (11), *i.e.* φ_4, can be neglected, it is concluded that the real roots of Eq. (11) exist only in the ranges where the sign of $f\bar{f}$ is same as that of $H\bar{H}$ because of $\varphi_2 \geqq 0$.

The natural frequency—the rotating speed diagram of the apparatus of the experiment IV for $\Delta=\Delta_{ij}=0$ is illustrated in Fig. 5 where the curves $f=0$ and $\bar{f}=0$ are shown by full and broken line curves respectively. Further the lines $H=0$ ($p=\pm 1$) and $\bar{H}=0$ ($\bar{p}=2\omega\pm 1$) are added by thin lines in Fig. 5. In Fig. 5 the real roots of Eq. (11) can exist only in blank regions and not in hatched regions where the signs of $f\bar{f}$ and $H\bar{H}$ are different each other. In the neighborhood of the cross point of $f=0$ and $\bar{f}=0$ shown by the symbol ○, there is an unstable region because the curves $\Phi'=0$ becomes as shown in Fig. 5 (a), (b), and near the intersecting points shown by the symbol ● in Fig. 5 (c) there is no unstable region[3]. The rotating speeds of ω of the intersecting points $C_1(\omega_{c1})$, $C_2(\omega_{c2})$, $D_{1,2}(\omega_d)$, and $A_{1,3}(\omega_a)$ are as follows[3]:

$$\begin{matrix}\omega_{c2}^2\\ \omega_{c1}^2\end{matrix} = \{(i_p - 1 - \delta) \pm \sqrt{(i_p-1+\delta)^2-4(i_p-1)\gamma^2}\}/2(i_p - 1) \tag{13}$$

$$\begin{matrix}\omega_d^2\\ \omega_a^2\end{matrix} = \{i_p^2 + 4(2 - i_p)(1 + \delta) \pm (4 - i_p)\sqrt{i_p^2 + 8(2 - i_p)(\delta - \gamma^2)}\}/8(2 - i_p)^2 \tag{14}$$

In the dynamic unstable region appearing in the neighborhood of ω_d, two unstable vibrations with frequencies p_1 and p_2 build up simultaneously and the amplitudes increase exponentialy as e^{mt}. The negative damping coefficient m takes its maximum value $m_{\max}$ at the center of unstable region $\omega=\omega_d$. The value of $m_{\max}$ and the width of unstable region $2|\xi_0|$ are approximately given by when there is no damping[3]

$$m_{\max} = \sqrt{-\varphi_2/\left(\frac{\partial f}{\partial p}\frac{\partial \bar{f}}{\partial \bar{p}}H\bar{H}\right)} = \nabla \tag{15-a}$$

$$2|\xi_0| = 4\nabla/\left| -\frac{\partial f}{\partial \omega}\Big/\frac{\partial f}{\partial p} + \frac{\partial \bar{f}}{\partial \omega}\Big/\frac{\partial \bar{f}}{\partial \bar{p}}\right| \tag{16-a}$$

when there is damping[5]

$$m_{\max} = \sqrt{\nabla^2 + \left(\frac{n_1 - n_2}{2}\right)^2} - \left(\frac{n_1 + n_2}{2}\right) \tag{15-b}$$

$$2|\xi_0| = 2\sqrt{\frac{(n_1 + n_2)^2}{n_1 n_2}\{\nabla^2 - n_1 n_2\}}\Big/\left| -\frac{\partial f}{\partial \omega}\Big/\frac{\partial f}{\partial p} + \frac{\partial \bar{f}}{\partial \omega}\Big/\frac{\partial \bar{f}}{\partial \bar{p}}\right| \tag{16-b}$$

where

$$\begin{gathered} n_1 = (n' + n'')_{p=p_1}, \quad n_2 = (n' + n'')_{p=p_2} \\ n' = \frac{\gamma^2 c_1}{2\gamma^2 + (1 - p^2)^2\left(2 - \frac{i_p\omega}{p}\right)}, \quad n'' = \frac{c_2}{\frac{2\gamma^2}{(1-p^2)^2} + \left(2 - \frac{i_p\omega}{p}\right)}. \end{gathered} \tag{17}$$

Putting $p=\bar{p}=\omega_c$, $n_1=n_2=(n'+n'')\omega_c$ in Eqs. (15), (16), (17), $m_{\max}$ and $2|\xi_0|$ of the static unstable vibrations appearing near the major critical speed ω_c are obtained.

4.2. Static unstable vibrations

The static unstable vibrations take place in the neighborhood of the intersecting points $C_1(p_1=\bar{p}_1)$ and $C_2(p_2=\bar{p}_2)$, because $H\bar{H}=(1-\omega_c^2)^2>0$ and hence the curves $\Phi'=0$ take the form of Fig. 5 (a). Eqs. (12-a), (15) and (16) show that m and $2|\xi_0|$ are functions of the orientation ζ and $\zeta=90°$ and $\zeta=0°$ furnish their minimum and maximum values when $QR>0$; vice versa when $QR<0$.

Since $QR=\varDelta\varDelta_S\omega_c^2(1-\omega_c^2)^2\{\gamma^2\omega_c^4+(\delta-\gamma^2)(1-\omega_c^2)^2\}$ is always positive for the flat shaft with uniform cross section ($\varDelta_{ij}\equiv\varDelta_s$), the following condition of removement of unstable region can be derived from $\varphi_2=0$, *i.e.* $Q=R(\zeta=90°)$:

$$\varDelta_s=\frac{\omega_c^2(1-\omega_c^2)^2\varDelta}{\gamma^2\omega_c^4+(\delta-\gamma^2)(1-\omega_c^2)^2} \tag{18}$$

For the apparatus of Fig. 2 (a) Eq. (18) furnishes $\varDelta_s=0.1$, $\varDelta=0.2493$ which agree with the result of Eq. (7). In order to obtain condition for removal of unstable region, Eq. (18) may be more convenient than Eq. (7). Incidentally, if the spring constant γ vanishes, *i.e.* $\gamma=0$, the motions of x, y and θ_x, θ_y do not couple each other, for such a system QR is always positive in the neighborhood of the higher major critical speed, *i.e.* the point C_1 because $QR=\delta\varDelta\varDelta_{22}\omega_c^2(1-\omega_c^2)^4>0$. For the apparatus of Fig. 2 with $QR>0$ the width of the unstable region $2|\xi_0|=\omega_{c22}-\omega_{c21}$ are plotted against the orientation ζ in Fig. 6 where the damping coefficient $c_1=c_2$ is adapted as a parameter. In Fig. 6, the results of approximate calculation through Eq. (16) are shown by full line curves and the exact values obtained from $|a_{ij}|=0$ of Eq. (4) are illustrated by the symbol ○; both results agree each other as is seen in Fig. 6. The existence of the fourth power term φ_4 in Eq. (11) which is assumed to be negligible gives plus effect on removal of the unstable region because $\varphi_4\geqq0$ and $-\varphi_2/H\bar{H}\leqq0$ in the neighborhood of the major critical speed.

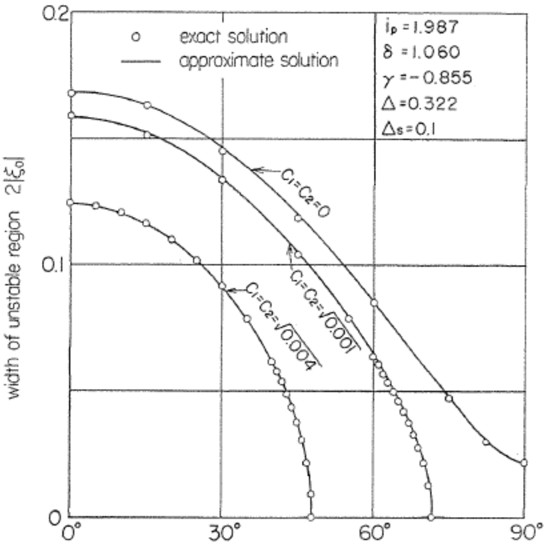

FIG. 6. $2|\xi_0|-\zeta$ diagram at ω_{c2}.

4.3. Dynamic unstable region

At the points $D_1(p_1=\bar{p}_2)$ and $D_2(p_2=\bar{p}_1)$, $H\bar{H}=(1-p_1^2)(1-p_2^2)$ takes a negative value, and hence there is an unstable region near D_1 and D_2 because the form of the curves $\Phi'=0$ becomes of Fig. 5 (b). The fourth power term $\varphi_4(\geqq 0)$ gives minus effect in this case because $-\varphi_2/H\bar{H}\geqq 0$. The negative damping coefficient m—the rotating speed ω diagrams with a parameter ζ for the system having $i_p=1$, $\delta=1.060$, $\gamma=-0.855$, $\Delta=0.3$, $\Delta_s=0.1$ and $c_1=c_2=0$ are shown in Fig. 7 (a). The relation between the maximum value of m, *i.e.*, m_{max} and the orientation ζ is given in Fig. 7 (b) where the symbol ○ is the exact results of Fig. 7 (a), the full line curve is of the approximate expression (15-a); the former is somewhat larger than the latter[3]. Since $QR<0$ in this case the value of m_{max} takes its maximum and minimum value at $\zeta=90°$ and $\zeta=0°$ separately, the relation of which is contrary to that of the static unstable vibration. For comparison the approximate value $m_{max}=0.1169$ and the exact value $m_{max}=0.1214$ of the system with $\Delta=0.3$ and $\Delta_s=0$ are illustrated by horizontal full and broken lines respectively in Fig. 7 (b). Incidentally the approximate value of m_{max} when $\Delta=0$, $\Delta_s=1$ is 0.0195, the result of which is not shown in the figure.

In general, the value of the orientation ζ has a remarkable effect on unstable

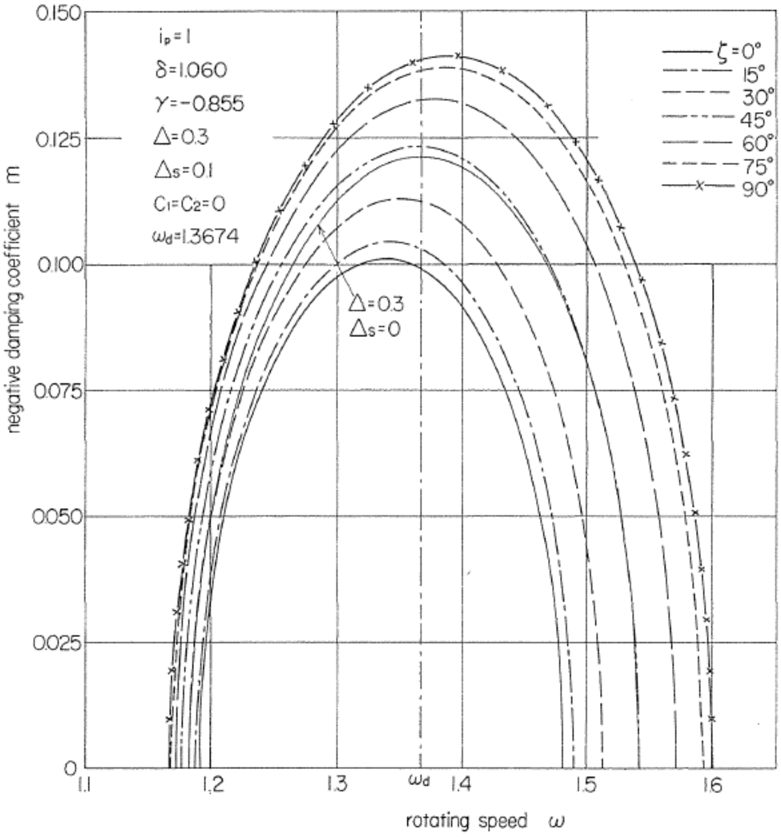

FIG. 7. (a) $m-\omega$ diagram at ω_d.

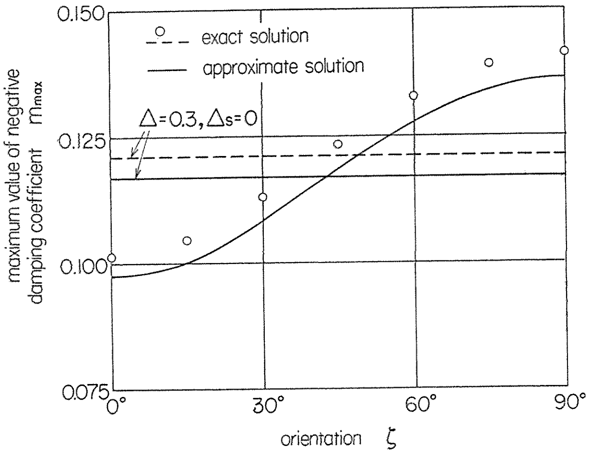

$(i_p=1,\ \delta=1.060,\ \gamma=-0.855,\ \Delta=0.3,\ \Delta_s=0.1,\ c_1=c_2=0)$

FIG. 7. (b) $m_{max}-\zeta$ diagram at ω_d.

vibrations appearing near both ω_c and ω_d, and m_{max} and the width $2|\xi_0|$ which are approximately proportional to $\sqrt{\varphi_2}=\sqrt{Q^2+R^2+2QR\cos 2\zeta}$ take their maximum and minimum values at $\zeta=0°$ and $\zeta=90°$ when $QR>0$, vice versa when $QR<0$.

5. Conclusions

Obtained conclusions may be summed up as follows:

(1) In damped systems as well as in systems without damping, the approximate analytical values of the width of unstable region $2|\xi_0|$, the negative damping coefficient m of the unstable vibrations agree well with their exact values.

(2) The values of $2|\xi_0|$ and m_{max} of unstable vibrations appearing at both ω_c and ω_d are proportional to the magnitude of $\sqrt{\varphi_2}=\sqrt{Q^2+R^2+2QR\cos 2\zeta}$ and the value of QR becomes positive or negative according to dimensions of apparatus and whether $\omega=\omega_c$ or ω_d. If $QR>0$, φ_2 takes its maximum and minimum values at $\zeta=0°$ and $\zeta=90°$ respectively, vice versa if $QR<0$. Incidentally for case of $\gamma=0$ or case of the flat shaft having $\Delta_{ij}\equiv\Delta_s$, QR at ω_c is always positive.

(3) By means of an appropriate combination of Δ and Δ_{ij} so that $|Q|=|R|$ and $\cos 2\zeta=-QR/|QR|$, φ_2 becomes equal to zero, and hence the unstable vibrations at ω_c are removed perfectly and they at ω_d can almost vanish even though there is the term of φ_4.

(4) Even when the static unstable region at ω_c vanishes by large enough damping and the steady forced vibrations take place, the orientation ζ has large effect on the response curves of the forced vibrations. This effect is similar to that on unstable region when $c_1=c_2=0$.

References

1) T. Yamamoto and H. Ōta, "On the Vibrations of the Shaft Carrying an Asymmetrical Rotating Body". Bulletin of the Japan Society of Mechanical Engineers, Vol. 6, No. 21, 1963, pp. 29-36.

2) T. Yamamoto and H. Ōta, "On the Forced Vibrations of the Shaft Carrying an Unsymmetrical Rotating Body (Response Curves of the Shaft at the Major Critical Speeds)", Bulletin of the Japan Society of Mechanical Engineers, Vol. **6**, No. 23, 1963, pp. 412-420.
3) T. Yamamoto and H. Ōta, "On the Unstable Vibrations of a Shaft Carrying an Unsymmetrical Rotor". Journal of Applied Mechanics, Trans. of the ASME, Vol. **31**, Series E, No. 3, 1964, pp. 515-522.
4) S. H. Crandall, and P. J. Brosens, "On the Stability of Rotation of a Rotor With Rotationally Unsymmetric Inertia and Stiffness Properties", Journal of Applied Mechanics, Vol. **28**, Trans. ASME, Vol. **83**, Series E, 1961, pp. 567-570.
5) T. Yamamoto and H. Ōta, "The Damping Effect on Unstable Whirlings of a Shaft Carrying an Unsymmetrical Rotor", Memoirs of the Faculty of Engineering, Nagoya University, Vol. **19**, No. 2, 1967, pp. 197-217.